

**CHARACTERIZATION OF PYROCLASTIC DEPOSITS AT KILBOURNE HOLE USING HANDHELD AND FIELD PORTABLE GEOCHEMICAL INSTRUMENTS.** C. A. Knudson<sup>1,2,3</sup>, A. M. Baldrige<sup>4</sup>, B. Harte<sup>4</sup>, Z. R. Morse<sup>1</sup>, C. N. Achilles<sup>1</sup>, A. D. Rogers<sup>5</sup>, L. A. Edgar<sup>6</sup>, P. Whelley<sup>1,2,3</sup>, A. C. McAdam<sup>1</sup>, C. I. Honniball<sup>1</sup>, K. E. Young<sup>1</sup>, T. D. Glotch<sup>5</sup>. <sup>1</sup>NASA Goddard Space Flight Center, Greenbelt, MD. (christine.a.knudson@nasa.gov), <sup>2</sup>University of Maryland College Park, MD. <sup>3</sup>Center for Research in Space Science & Technology II (CRESST II), Greenbelt, MD. <sup>4</sup>St. Mary's College, Moraga, CA. <sup>5</sup>Stony Brook University, Stony Brook, NY. <sup>6</sup>USGS Astrogeology Science Center, Flagstaff, AZ

**Introduction:** Handheld and field portable geochemical instruments were utilized for *in situ* measurements of pyroclastic deposits on the North rim of Kilbourne Hole in the Potrillo Volcanic Field in Southern New Mexico. These measurements were taken to support goals laid out in the Remote In Situ Synchrotron Studies for Science and Exploration 2 (RISE2) node of the Solar System Exploration Virtual Research Institute (SSERVI). Here, we present the geochemical and mineralogical data collected with three of those instruments at select locations within Kilbourne Hole. This maar formed during a phreatomagmatic eruption, and the layered deposits here overlay paleosols associated with the Camp Rice Formation and the Afton basalt [1].

**Field Work & Data Acquisition:** The RISE2 team deployed to Kilbourne Hole again in the fall of 2021 [2] to take coordinated measurements with multiple handheld and field portable instruments. Data discussed here are from a backpack mounted Analytical Spectral Devices Inc. (ASD) FieldSpec spectroradiometer (0.3–2.5  $\mu\text{m}$ ), and two handheld instruments; a SciAps handheld Laser Induced Breakdown Spectrometer (hLIBS) and a SciAps handheld X-ray fluorescence (hXRF) spectrometer [2] at two different vertical sections on the North rim of Kilbourne Hole, however additional field portable/handheld instruments were also deployed [2,3]. Both the hLIBS and the hXRF provide elemental data which have been converted into oxide weight percentages, while the ASD is capable of identifying primary and secondary minerals/mineral groups based on reflectance spectra.

The three instruments took *in situ* measurements at 47 different locations along the first marked section (Fig. 1). and 11 different locations at the second marked section (Fig. 2), located just to the East of the first section. Care was taken to ensure that all three instruments were taking the measurements in the same sample location so that data can be compared [2]. Five hLIBS shots, one hXRF shot, and one ASD measurement were acquired at every marked location. More hLIBS shots were acquired to account for the smaller spot size (compared to the hXRF and ASD). Acquisition of ASD data utilized the artificially illuminated contact probe to avoid complications from scattered light or atmospheric irregularities.



Figure 1. Top portion of the pyroclastic sequence on the North rim of Kilbourne Hole. Measurements were taken from a red marker flag at the bottom of the section to the top, shown here, each analyzed spot was marked.



Figure 2. The second pyroclastic sequence on the North rim of Kilbourne Hole, located to the East of the first section.

**Results:** Elemental data from both the hXRF and the hLIBS were converted to oxide weight percent, normalized, and plotted as a function of location on the outcrop (from bottom to top). The five hLIBS shots are also averaged to reduce input from outliers (e.g., shots that may have hit only a single mineral grain). Raw ASD data were converted to reflectance (the ratio of the total amount of radiation reflected by a surface to the total amount of radiation incident on the surface) using ASD

commercial software ViewSpec Pro, which utilized white calibration panel measurements taken throughout data acquisition. The VNIR outcrop transects were plotted in ENVI and stacked similar to hyperspectral imagery which allowed rapid assessment and characterization of mineralogical differences in the vertical sections using ENVI visualization techniques (e.g. decorrelation stretch, three-band images) [4]. Trends in the measurements or unique measurements could then be analyzed further. This was particularly useful because the spectra on initial visual inspection show very little difference. An example of one such “spectral cube” is given in Figure 3.

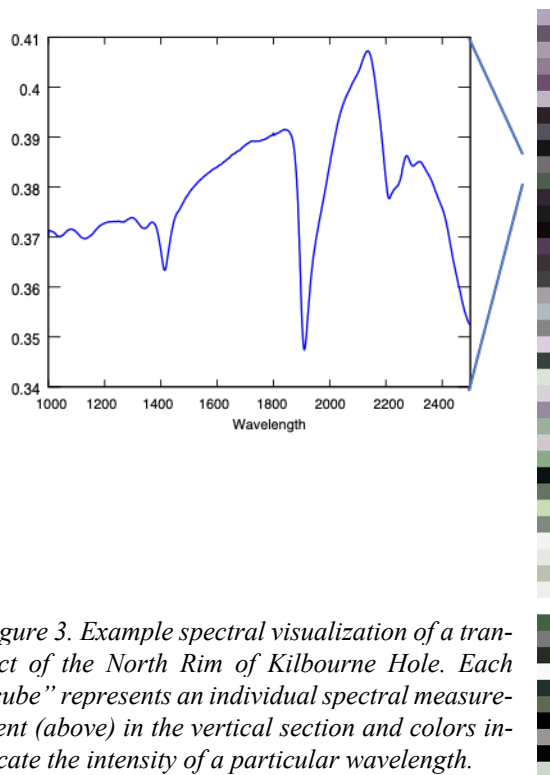


Figure 3. Example spectral visualization of a transect of the North Rim of Kilbourne Hole. Each “cube” represents an individual spectral measurement (above) in the vertical section and colors indicate the intensity of a particular wavelength.

**North Rim Section 1:** While there are not large variations in major element composition moving from the bottom to the top of the Northern most section, some trends can be pulled from the hXRF data set. MgO and CaO are most abundant in the middle of the section and there is little variation in SiO<sub>2</sub> in the middle portion of the section, while Al<sub>2</sub>O<sub>3</sub> is more variable in the top and bottom of the section.

Additionally, major elements from the hLIBS data set for this section do not show large variations in either, however because the hLIBS spot size is much smaller than the hXRF spot size some of the observed variation in major element abundances could be a result of the

instrument hitting a single mineral grain, rather than the representative “bulk” deposit. This is taken into consideration during data interpretation. Na<sub>2</sub>O is slightly less abundant in the middle of the section, while MgO is slightly elevated in the upper section. Both CaO and Al<sub>2</sub>O<sub>3</sub> seem fairly constant throughout the section.

The VNIR spectra are consistent with the presence of montmorillonite with an additional smectite clay. Variation is primarily found in the Al-OH and Fe and Mg-OH related features near 2200 nm and 2300 nm with these features most prominent in the mid-section of the outcrop. These observations correlate well with the elevated MgO and CaO in the middle of the section identified with the hXRF measurements.

**North Rim Section 2:** In the second section, hXRF results show that both MgO and CaO increase from bottom to top, while Al<sub>2</sub>O<sub>3</sub> shows very little variation, except in points 5 in the middle of the section (higher Al<sub>2</sub>O<sub>3</sub>) and 11 at the top of the section (lower Al<sub>2</sub>O<sub>3</sub>). SiO<sub>2</sub> varies throughout the section with notably lower SiO<sub>2</sub> at point 5.

hLIBS data from the second section show elevated CaO and K<sub>2</sub>O, and lower Na<sub>2</sub>O and Fe<sub>2</sub>O<sub>3</sub><sup>T</sup> at the top of the section (point 11) while points 9 and 10 have higher Na<sub>2</sub>O and Fe<sub>2</sub>O<sub>3</sub><sup>T</sup> and lower CaO and K<sub>2</sub>O. There is not much variation in Al<sub>2</sub>O<sub>3</sub> in this section.

VNIR data collected with the ASD show similar mineralogy in this section as in the first, with less variation in the Fe and Mg related wavelengths.

**Future Work:** RISE2 work will continue with additional field deployments in the Spring of 2023, and while the focus of these additional deployments is on simulated extravehicular activities and astronaut training procedures [2,5,6] time should allow for additional measurements at these same sections to be acquired and/or additional sequences to be identified and *in situ* measurements can be taken to add to this data set if needed.

**Acknowledgments:** The authors would like to acknowledge RISE2 funding through NASA NRA# NNH18ZDA018C.

**References:** [1] Reiche, P. (1940) *American Journal of Science*, v.238, 212-255. [2] Knudson C. A. et al. (2022) *LPSC #1725*. [3] Rogers A. D. et al. (2023) *LPSC, Abstract #2162*. [4] Calvin, W. et al., (2010) *GRC Transactions*, 34, 761-764. [5] Young, K. E. et al. (2020) *Lunar Surface Science Workshop, LPI Cont. No.2241*, id.5143. [6] Morse, Z. R. et al. (2023) *LPSC, this conference*.